Evolution of auroral asymmetries in the conjugate hemispheres during two substorms

N. Østgaard,[1] B. K. Humberset,[1] and K. M. Laundal[1]

Received 4 November 2010; revised 2 December 2010; accepted 13 December 2010; published 1 February 2011.

[1] Five hours of simultaneous global imaging data from the conjugate hemispheres are used to examine the dynamics of the auroral substorm. Earlier studies have demonstrated that substorm onset locations in the two hemispheres are systematically displaced due to the orientation of the interplanetary magnetic field. In this paper we present, for the first time, how the asymmetric auroras induced by the IMF orientation at substorm onset disappears during the expansion phase. We suggest that this is the large scale manifestation of auroral arcs as being the sites of magnetic stress release. Magnetic stress on field lines with asymmetric footpoints can lead to a net hemispherical difference in parallel electric field strength which implies that the auroras move with different speeds in the two hemispheres to release the magnetic stress. The relative velocity can be derived from the potential between the hemispheres. During expansion phase the twisted magnetic fields are rectified, bringing the closed magnetic field lines back to the configuration defined by the Earth's interior.
Citation: Østgaard, N., B. K. Humberset, and K. M. Laundal (2011), Evolution of auroral asymmetries in the conjugate hemispheres during two substorms, *Geophys. Res. Lett.*, *38*, L03101, doi:10.1029/2010GL046057.

1. Introduction

[2] We have previously reported that the locations of the auroral substorm onset in the conjugate hemispheres are usually not symmetric [*Østgaard et al.*, 2004, 2005]. The degree of asymmetry is strongly correlated with the orientation of the Interplanetary Magnetic Field (IMF) or more precisely the IMF clock angle (θ_c), that is, the angle between the IMF and the Z-axis in the YZ plane of the Geocentric Solar Magnetospheric (GSM) reference system. This IMF θ_c control can be understood as the magnetic stress imposed by the IMF on the Earth's magnetic field from the moment the field lines are opened on the dayside, draped down the tail and until they eventually close through reconnection in the mid-tail before substorm onset. The result of this tension force on open field lines is that only field lines with asymmetric footpoints will reconnect in the mid-tail [*Østgaard et al.*, 2005] forming closed field lines with asymmetric footpoints. One could also consider the asymmetric cross-tail pressure resulting from a non-zero IMF B_y to explain the partly penetration of IMF B_y into the closed magnetosphere [*Khurana et al.*, 1996]. At the substorm onset energetic electrons travel from the source region in the magnetotail on a time scale (~ 1 s) much shorter than any motion due to plasma convection. The auroral arcs can therefore be considered to be the illuminated footpoints of the magnetic field lines connecting the two hemispheres. Asymmetric footpoints means that these field lines are twisted. This strong IMF θ_c control of the asymmetry of the substorm onset locations was further supported by a statistical analysis [*Østgaard et al.*, 2007]. Although, some studies have used B_y instead of θ_c to organize the substorm onset locations [e.g., *Wang et al.*, 2007], we consider that the asymmetry of substorm onset locations, due to the magnetic stress on open field lines or the partly penetration of the IMF B_y into the magnetosphere, is fairly well documented. The observed asymmetry is also larger than predicted by the empirical magnetic field models [*Østgaard et al.*, 2005].

[3] Conjugate auroral imaging data have been used to address the asymmetry of open-closed boundaries [*Stubbs et al.*, 2005; *Laundal et al.*, 2010] and auroral features [*Stenbaek-Nielsen et al.*, 1972; *Laundal and Østgaard*, 2009] during substorms. In this paper we take the investigations of interhemispherical differences one step further, by studying, for the first time, the global evolution of the longitudinal asymmetries in the substorm auroras.

2. Data

[4] On October 22, 2001, the Polar and IMAGE satellites recorded 5 hours of continuous global conjugate imaging data capturing two subsequent auroral substorms. IMAGE - WIC [*Mende et al.*, 2000] (Lyman-Birge-Hopfield band: 140–180 nm) imaged the evolution of the auroral substorm in the northern hemisphere, while Polar VIS Earth camera [*Frank et al.*, 1995] (124–149 nm and dominated by the atomic oxygen (O I) line at 130.4 nm) imaged the southern hemisphere. The OI-emissions measured by VIS Earth camera are slightly more scattered than the N2 and N emissions measured by WIC, and the emission intensity also varies with energy [*Frey et al.*, 2003]. As we look at relatively large similar features in both hemispheres to determine if and how much they are displaced relative to each other in local time, we do not believe that the different wavelengths of the two cameras bias our results. Exposure times are 10 s and 32.5 s and cadence is ~2 min and 1 min for IMAGE WIC and VIS Earth camera, respectively. We assume the emission height to be 130 km and map the images onto magnetic apex coordinates [*Richmond*, 1995]. This coordinate system is based on the International Geomagnetic Reference Field and does not take into account any asymmetries imposed by external fields. The mapping accuracy is dependent on the pointing accuracy of the instruments. In addition to the usual star calibration, we have used available DMSP passes to confirm that we have a spatial accuracy of about 1°–2°. The IMF measurements are provided by WIND located at [34,1,2]

[1]Department of Physics and Technology, University of Bergen, Bergen, Norway.

0094-8276/11/2010GL046057

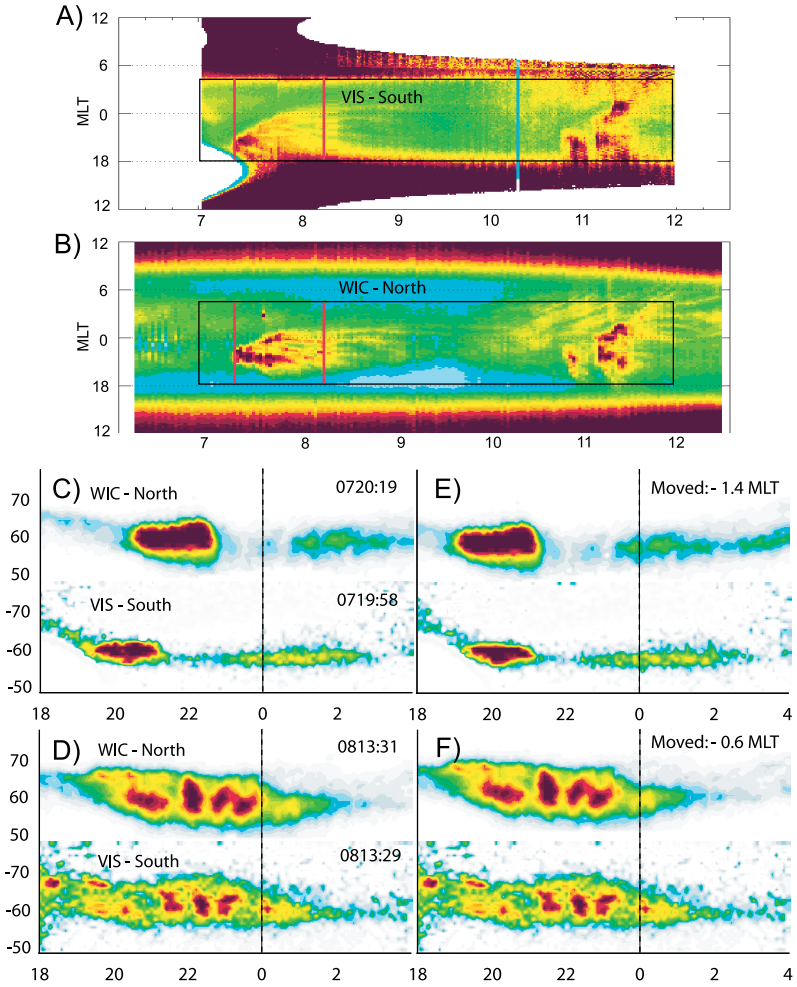

Figure 1. (a) Keogram of the emissions in the southern hemisphere from 7 UT to 12 UT on October 22, 2001 (VIS). Emissions are integrated between 65° and 85° and plotted every minute. (b) Keogram from the northern hemisphere every two minutes (WIC). (c) A pair of original images. (e) The same images after the 2D correlation method has been applied. (d, f) Similar to Figures 1c and 1e later in the substorm. Colors are normalized to substorm onset. A movie showing all the images is given in the auxiliary material.

R_E GSM. In order to examine any IMF influence on the inner night-side magnetosphere we have assumed a planar propagation of the solar wind to −10 R_E [*Østgaard et al.*, 2004].

3. Results

[5] In Figures 1a (southern hemisphere) and 1b (northern hemisphere) we show the 5-hour time interval of simultaneous imaging observations as keograms of integrated emissions between 65° and 85° plotted every one (two) minute for VIS (WIC). Color bars are chosen to match peak intensity at substorm onset. As the tilt angle during these observations varied between −20° and −10°, there is more dayglow in the southern than in the northern hemisphere. Although most of this dayglow can be removed with a fairly robust method the dayglow removal may introduce some artificial differences in intensities. To avoid this we restrict our analysis to only compare features between 18 MLT and 04 MLT from 07 UT until 1140 UT. This time interval contains one substorm at 0716 UT, a pseudo-breakup at 1044 UT and a new substorm at 1105 UT.

[6] We apply three different methods to determine asymmetric features; visual inspection, 1D correlation and 2D correlation. The visual inspection is carried out by overlaying each image on a grid with 0.2 MLT resolution, normalizing the intensities and determining edges and peaks (of intensities) for all the images with overlapping exposure times. The 1D and 2D correlation methods were carried out in two steps. First, after dayglow removal, each image was converted onto a rectangular grid with 0.1 magnetic local time and 1° magnetic latitude resolution giving a matrix, 160 × 30, covering 18-4 MLT and 50°–80° magnetic latitude. WIC and VIS images with no more than 1 minute time difference (center time of exposure) are compared. Two examples are shown in Figures 1c and 1d. For the 1D correlation method, all the counts between 50° and 80° magnetic latitude are added and the two resulting vectors are cross correlated with shifts from −3 MLT to +3 MLT. For the 2D correlation method we calculated

$$\chi^2(i,j) = \frac{\sum_x \sum_y [WIC(x+i, y+j) - VIS(x,y)]^2}{\sum_x \sum_y WIC(x+i, y+j)^2} \quad (1)$$

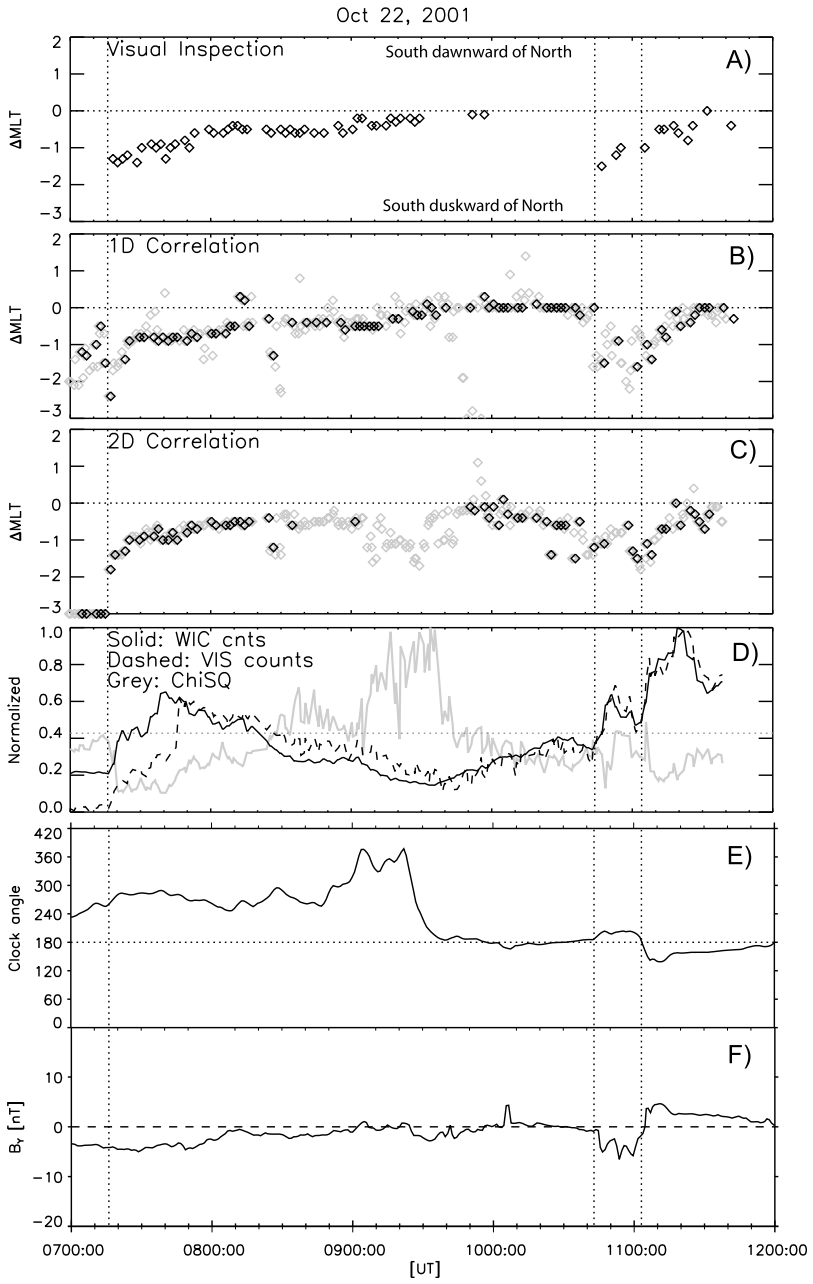

Figure 2. The relative displacement, ΔMLT, of substorm auroral features based on (a) visual inspection, (b) 1D cross correlation, (c) 2D correlation. Grey diamonds are all data, black diamonds are valid data. (d) Normalized total counts in WIC (solid line) and VIS (dashed line) images and minimum χ^2 (grey line). (e) IMF θ_c and (f) IMF B_y from WIND at [34,1,2] R_E GSM, planar propagated to −10 R_E.

where x and y have 0.1 MLT and 1° latitude resolution and we let i vary from −30 to +30 (±3 MLT) and j vary from −8 to +8 (±8°). In Figures 1e and 1f we show the shifted (in i,j) WIC image that returned the smallest $\chi^2(i,j)$. A movie showing all the images is given in the auxiliary material.[1]

[7] Figure 2a–2c show the result from applying the three different methods, as well as the IMF θ_c and B_y (Figures 2e and 2f).

[8] For the 1D and 2D correlations the grey diamonds are all the compared images with no more than 1 minute time difference. The black diamonds in Figure 2b are data where the images are overlapping in time (center times differ < 21 s) and correlation coefficient > 0.4. The black diamonds in Figure 2c are data where the images are overlapping in time and $\chi^2 < 0.4$, normalized value, as marked by horizontal grey dashed line in 2D. For both substorms the first brightening is asymmetric consistent with earlier findings. Then, all the methods show that the asymmetry disappears during the expansion phase. The 2D method also indicates that the

[1] Auxiliary materials are available in the HTML. doi:10.1029/2010GL046057.

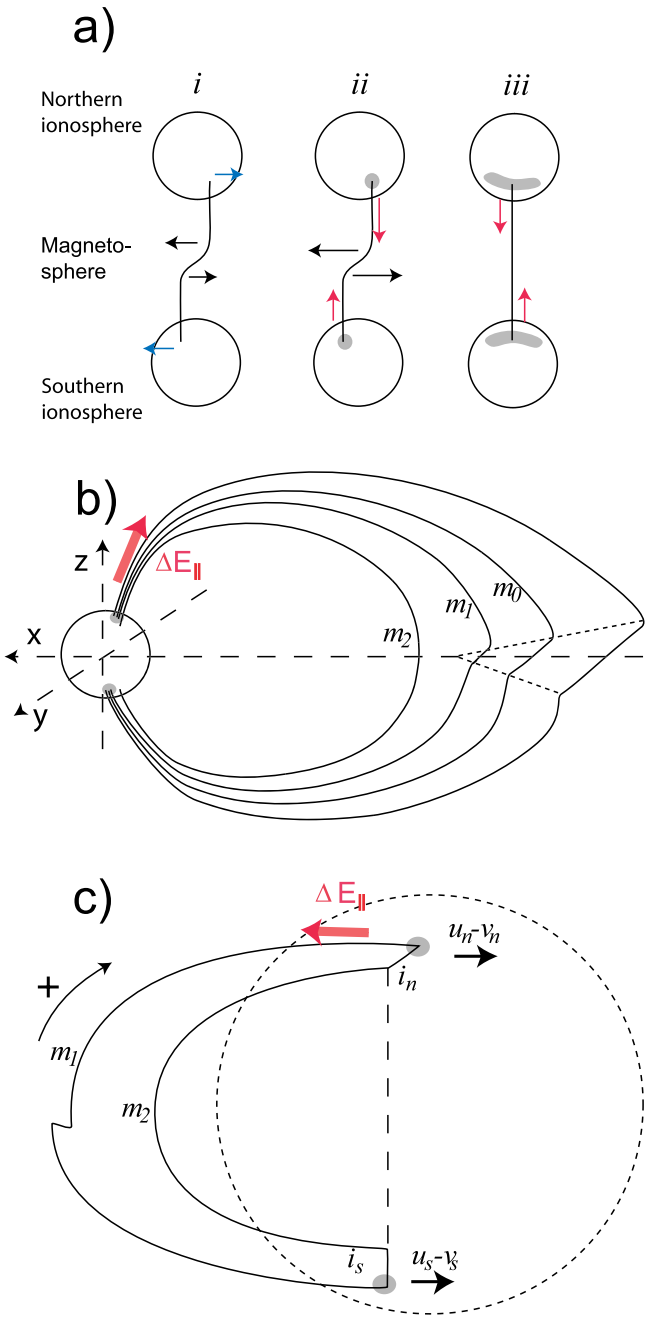

Figure 3. (a) How the field line is rectified due to magnetic stress (black arrows) on field lines with asymmetric footpoints. Blue arrows indicate ionospheric friction and red arrows parallel electric fields. (b) How the magnetic fields are twisted from the tail and inward with a non-twisted field line earthward of the onset region. (c) A loop of the twisted field line m_1 with asymmetric footpoints and the non-twisted inner field line, m_2 with symmetric footpoints. $\Delta E_{||}$ is the net difference between the two hemispheres on the twisted field line. The two ionospheric segments, i_n and i_s, complete the loop, and u and v are the speeds of the loop and the plasma, respectively, defined positive eastward.

asymmetry recurs during the weak precipitation before the pseudo-breakup (1044 UT).

4. Discussion and Summary

[9] Neither the IMF B_y or θ_c can account for the asymmetry changes. The variations in IMF B_y are small, and during the first 10 minutes of the first substorm ΔMLT changes ~1 hour while B_y stays constant. During the second substorm the IMF B_y turns positive without inducing an opposite asymmetry. The correlation coefficient between IMF B_y and ΔMLT is only 0.5 and 0.4 for the 1D and 2D method, respectively, when the 'good' data (black diamonds) are used. The θ_c stays fairly constant for the first substorm except after 9 UT when both B_y and B_z (not shown) are very close to zero.

[10] *Haerendel* [2007] has suggested that the immediate source of auroral energy is the magnetic shear stresses, which 'are set up by longitudinal convection driven by pressure forces in the outer magnetosphere against the frictional forces in the lower ionosphere'. Furthermore, that the 'release of these stresses are enabled by the "cutting" of field lines' [*Haerendel*, 2007], often described as the decoupling of the magnetosphere from the ionosphere due to parallel potential drops. In this scenario the auroral arcs will move in the direction of releasing magnetic stress. We suggest that our observations are a large scale manifestation of this effect. A simple sketch of this scenario is depicted in Figure 3a. Due to the stress imposed on the open field lines by the negative IMF B_y ($\theta_c = 240°$) the closed magnetic field lines before substorm onset have asymmetric footpoints (Figure 3a, left). The resulting magnetic stress on this closed field line (black arrows) is balanced by ionospheric friction (blue arrows). At substorm onset (Figure 3a, middle) the field lines are dipolarized, which increases the magnetic field strength and the tension force in the tail (larger black arrows) and, if overcoming the frictional force in the ionosphere, this will act to decrease the asymmetry. However, parallel electric fields are also created which will decouple the magnetic field in the ionosphere, allowing the field lines to 'slip' back to the symmetric configuration defined by the Earth's interior field (Figure 3a, right).

[11] A simple theoretical argument can be made.

[12] First, we apply Ampere's law to this problem [see, e.g., *Stenbaek-Nielsen and Otto*, 1997]. While the magnetic stress associated with tail stretching implies pairs of upward/downward field aligned currents (FAC), a twist in B_y implies an interhemispheric FAC

$$\left(\frac{\partial B_y}{\partial x}\right)_{||} \sim \mu_0 j_{||} \tag{2}$$

Combined with a finite conductivity, most likely in the acceleration region as depicted in Figures 3b and 3c, this implies a net potential ($\Delta E_{||}$) between the hemispheres. Considering now that the twist is produced in the tail decreasing steadily towards the Earth, as depicted in Figure 3b, the left term in equation (2) is negative, which implies that $\Delta E_{||}$ is pointing southward (along m_1). There are of course parallel electric fields in the acceleration regions in both hemispheres, but for simplicity we only consider the net difference between the two hemispheres. Along m_2 there is no $\Delta E_{||}$ as $\frac{\partial B_y}{\partial x} = 0$.

[13] Now, we apply Faraday's law along a loop of the two closed magnetic field lines (m_1 and m_2) and the two small segments (i_n and i_s) in the ionosphere connecting them, as shown in Figure 3c.

$$\oint (\mathbf{E} + \mathbf{u} \times \mathbf{B}) \cdot d\mathbf{l} = -\frac{d}{dt} \int \mathbf{B} \cdot d\mathbf{A} \tag{3}$$

where $\mathbf{u}$ is the speed of the loop. This approach was originally proposed by *Vasyliunas* [1984] choosing a loop along field lines at the separatrix to estimate the reconnection electric field. *Laundal et al.* [2010] extended this approach to show that parallel electric fields could lead to relative motion of of magnetic footpoints in the two hemispheres. Following *Vasyliunas* [1984] we let the loop move with the magnetic field line, which implies that no magnetic field lines cross the surface encircled by the loop and the right side of equation (3) equals zero. We let the ionospheric segments be at altitudes where the MHD approximation ($\mathbf{E} + \mathbf{v} \times \mathbf{B} \approx \mathbf{0}$) holds. This altitude has to be below the acceleration region (1-2R_E) and above the altitude where the ratio of electron-neutral collision frequency and gyrofrequency is small.

[14] Considering also the segment l with parallel electric field (along m_1) equation (3) becomes

$$\int_{m_1} \left[\Delta \mathbf{E}_{\parallel} + (\mathbf{u} - \mathbf{v}) \times \mathbf{B}\right] \cdot d\mathbf{l} + \int_{i_n, m_2, i_s} \left[(\mathbf{u} - \mathbf{v}) \times \mathbf{B}\right] \cdot d\mathbf{l} = 0 \tag{4}$$

As the integration path is along the magnetic field lines the only contribution along m_1 comes from the net parallel electric field and the integral along m_2 is zero. By defining (u-v) positive eastward in both hemispheres and noticing that the magnetic field is upward (downward) in the South (North) we get

$$-\Delta E_{\parallel} l - (u_n - v_n) B_n i_n + 0 + (u_s - v_s) B_s i_s = 0 \tag{5}$$

Following *Laundal et al.* [2010] we assume the convection speed in the two hemispheres to be equal ($v_n = v_s$) as well as the length of the two ionospheric segments ($i_n = i_s = L$) and the magnetic field strength in the two ionospheres ($B_n = B_s = B$). Then, we get

$$u_s - u_n = \frac{\Delta E_{\parallel} l}{BL} \tag{6}$$

This shows that the motion of the magnetic footpoints in southern hemisphere will be faster than in the northern hemisphere as long as there is a $\Delta E_{\parallel}$ pointing southward. Eventually, this relative speed difference will re-establish symmetric footpoints by rectifying the field line and release the magnetic stress ($\frac{\partial B_y}{\partial x} \neq 0$) that created $\Delta E_{\parallel}$ in the first place. This result applies to the region where $\frac{\partial B_y}{\partial x} \neq 0$ at the outer field line and $\frac{\partial B_y}{\partial x} = 0$ at the inner field line. If we had chosen a loop along a field line tailward of the onset region and assuming that $\frac{\partial B_y}{\partial x}$ is constant at m_1 and m_0 (Figure 3b), the $\Delta E_{\parallel}$ along the two segments would cancel in the integration and $u_s = u_n$.

[15] In the case of $\Delta E_{\parallel} = 0$, which might be the condition before onset, the asymmetry would not change. This is consistent with what we see prior to 1042 UT.

[16] Another implication of this result is that the aurora should be brighter in the northern hemisphere (in our case) if the strength of the $\Delta E_{\parallel}$ is comparable to, or at least a substantial fraction of the potential drops in the acceleration regions. As we are looking at different wavelengths with different cameras we are not able to address this. However, this could explain the brightness differences reported by *Frank and Sigwarth* [2003]. With the southern onset being dawnward of the northern, the twist was opposite of what we see, resulting in a $\Delta E_{\parallel}$ pointing northward. Thus, a brighter aurora should be seen in the South, which is what they did.

[17] To summarize, in this paper we have reported the following:

[18] 1. Both substorm onsets are asymmetric - due to the magnetic stress imposed by the IMF on opened magnetic field or the partial penetration of IMF B_y.

[19] 2. During the expansion phase of both substorms the asymmetry disappears.

[20] Our findings can be explained by the decoupling of the magnetosphere and ionosphere due to parallel electric fields that are produced in the substorm process allowing the field lines to 'slip' back to the symmetric configuration defined by the Earth's interior.

[21] We have also presented a theoretical argument:

[22] 1. The magnetic stress on field lines with asymmetric footpoints can set up a net difference in parallel electric field in the two hemispheres.

[23] 2. This net electric field difference will lead to a different speed of the auroral arcs in the two hemispheres rectifying the magnetic field lines and releasing magnetic stress.

[24] The overall result is that the closed magnetic field lines are brought back to what the Earth's interior determines.

[25] **Acknowledgments.** We thank S. B. Mende for the use of IMAGE FUV WIC data, J. B. Sigwarth for the use of Polar VIS Earth Camera data and R. Lepping for the WIND magnetic field data. This study was supported by the Norwegian Research Council, through the IPY-ICESTAR project 176045/S30.

References

Frank, L. A., and J. B. Sigwarth (2003), Simultaneous images of the northern and southern auroras from the Polar spacecraft: An auroral substorm, *J. Geophys. Res.*, *108*(A4), 8015, doi:10.1029/2002JA009356.

Frank, L. A., J. B. Sigwarth, J. D. Craven, J. P. Cravens, J. S. Dolan, M. R. Dvorsky, P. K. Hardebeck, J. D. Harvey, and D. W. Muller (1995), The visible imaging system (VIS) for the Polar spacecraft, *Space Sci. Rev.*, *71*, 297–328.

Frey, H. U., S. B. Mende, T. J. Immel, J. C. Gérard, B. Hubert, J. Spann, G. R. Gladstone, D. V. Bisikalo, and V. I. Shematovich (2003), Summary of quantitative interpretation of IMAGE ultraviolet auroral data, *Space Sci. Rev.*, *109*, 255–283.

Haerendel, G. (2007), Auroral arcs as sites of magnetic stress release, *J. Geophys. Res.*, *112*, A09214, doi:10.1029/2007JA012378.

Khurana, K. K., R. J. Walker, and T. Ogino (1996), Magnetospheric convection in the presence of interplanetary magnetic B_y: A conceptual model and simulations, *J. Geophys. Res.*, *101*(A3), 4907–4916.

Laundal, K. M., and N. Østgaard (2009), Asymmetric auroral intensities in the Earth's Northern and Southern hemispheres, *Nature*, *460*, 491–493, doi:10.1038/nature08154.

Laundal, K. M., N. Østgaard, K. Snekvik, and H. U. Frey (2010), Interhemispheric observations of emerging polar cap asymmetries, *J. Geophys. Res.*, *115*, A07230, doi:10.1029/2009JA015160.

Mende, S. B., et al. (2000), Far ultraviolet imaging from the IMAGE spacecraft: 2. Wideband FUV imaging, *Space Sci. Rev.*, *91*, 271–285.

Østgaard, N., S. B. Mende, H. U. Frey, T. J. Immel, L. A. Frank, J. B. Sigwarth, and T. J. Stubbs (2004), Interplanetary magnetic field control of the location of substorm onset and auroral features in the conjugate hemispheres, *J. Geophys. Res.*, *109*, A07204, doi:10.1029/2003JA010370.

Østgaard, N., N. A. Tsyganenko, S. B. Mende, H. U. Frey, T. J. Immel, M. Fillingim, L. A. Frank, and J. B. Sigwarth (2005), Observations and model predictions of substorm auroral asymmetries in the conjugate hemispheres, *Geophys. Res. Lett.*, *32*, L05111, doi:10.1029/2004GL022166.

Østgaard, N., S. B. Mende, H. U. Frey, J. B. Sigwarth, A. Aasnes, and J. M. Weygand (2007), Auroral conjugacy studies based on global imaging, *J. Atmos. Terr. Phys.*, *69*, 249–255, doi:10.1016/j.jast9.2006.05.026.

Richmond, A. D. (1995), Ionospheric electrodynamics using magnetic apex coordinates, *J. Geomagn. Geoelectr.*, *47*, 191–212.

Stenbaek-Nielsen, H. C., and A. Otto (1997), Conjugate auroras and the interplanetary magnetic field, *J. Geophys. Res.*, *102*, 2223–2232.

Stenbaek-Nielsen, H. C., T. N. Davis, and N. W. Glass (1972), Relative motion of auroral conjugate points during substorms, *J. Geophys. Res.*, *77*, 1844–1852.

Stubbs, T. J., R. R. Vondrak, N. Østgaard, J. B. Sigwarth, and L. A. Frank (2005), Simultaneous observations of the auroral ovals in both hemispheres under varying conditions, *Geophys. Res. Lett.*, *32*, L03103, doi:10.1029/2004GL021199.

Vasyliunas, V. M. (1984), Steady state aspects of magnetic field line merging, in *Magnetic Reconnection in Space and Laboratory Plasmas*, *Geophys. Monogr. Ser.*, vol. 30, edited by E. W. Hones Jr., pp. 25–31, AGU, Washington, D. C.

Wang, H., H. Lühr, S. Y. Ma, and H. U. Frey (2007), Interhemispheric comparison of average substorm onset locations: Evidence for deviation from conjugacy, *Ann. Geophys.*, *25*, 989–999.

B. K. Humberset, K. M. Laundal, and N. Østgaard, Department of Physics and Technology, University of Bergen, Allegt. 55, N-5007 Bergen, Norway. (nikolai.ostgaard@ift.uib.no)